YRHI-99-29

The Physics of the TPC Response Simulator

brian.lasiuk@yale.edu

A brief summary of the physics that is simulated in the TPC Response Simulator (TRS). This is taken from the TRS manual and user guide. This is intended to be a STAR Note in the future.

1 Overview and Design

The **TRS** design document[1] sets out the design, requirements and philosophy of **TRS**, as well as the first simple description of the algorithms proposed for use in the various processes that are modeled.

The initial prototyping phase led to the development of two types of classes that make up the core of the physics and simulation components of **TRS**:

- **Processes** – physical processes that model an aspect of the physics occuring in the chamber such as charge transport, wire chamber operation and signal generation. These are defined in detail in section 1.1.
- **Containers** – structures which contain the various types and forms of data required in the time evolution of the simulation.

In the class design of the package, each physical process, as described above, was mapped to a single class, as were the containers. This provides a simple factorization between processes which allows them to function independently of one another. It also allows the isolation of single processes for detailed study independent of the effect of other processes. As an example, previous attempts to simulate the behavior of a wire chamber use a parameterization (f) of a pad response function from empirical relations such as:

$$f(x) \sim e^{-(x-x_o)^2/(2\sigma^2)} \tag{1}$$

where σ incorporates terms which depend on the orientation of the trajectory of a particle, the transport properties of ionization through a gaseous medium, pad plane geometry, electronics properties, etc. As such it is very difficult to isolate the effects of a specific process, and parameters which affected by many different processes result. This reduces the physical significance of tunable parameters and while this may be fine for large scale production of data, for understanding of the effects of physical processes, it is not very useful. This does not need to be the case since the physics processes important in the operation of a TPC are independent of not only the granularity of the simulation but also the level of detail of the simulation. As an example, one needs to transport the ionization to the read-out plane independent of whether it is a single electron or segment of charge, however the detail of whether one calculates the drift velocity at every point on a fine mesh grid and propagate the charge across the grid, or do a simple projection of the charge onto the pad plane. As such, the above processes can define an interface from which the *FAST* parameterizations and the *SLOW* microscopic simulation can utilize. This allows the use of the same code and interface with only a switch (or flag) which can be used to set the detail of the simulation. This allows the same infrastructure to handle various levels of detail without resorting to separate packages for each. Rather the same interface will mean the same function names will be called, with only the implementations which vary.

As such, the **processes** are the actual physical events that occur inside the chamber and operate on data which are stored in **containers**. Thus a general practice was followed that input data would be passed to a **process** class via a **container** and the processor would either mutate the data within the containers or produce data that would be stored more

[1] http://www.rhic.bnl.gov/STAR/html/comp_l/simu/TpcRespSim/src/ps/TrsDesign.ps

naturally in a new or separate **container** for the next physics process. As such, although the functions of these two types of classes fulfill two different needs within the package, the relation between them is very close. These relations are explained in terms of very physical means in the following two sections (sections 1.1 and 1.2),

1.1 Physical Processes

There are four main types of **processes** that were identified as being necessary to model in order to reproduce the operation of a TPC in **TRS**. When discussing the mode of operation of a TPC they become evident:

- *Ionization Transport* – charge transport of the ionization. deposited in the active region to the readout chambers.
- *Charge Collection* – electron/ionization collection on the sense wires of the multi-wire proportional chamber (MWPC).
- *Analog Signal Generation* – charge induction on the pad plane and the generation of the time evolution of the analog signals on the pads.
- *Digital Signal Generation* – Digital conversion of analog signals.

A brief overview of the processes are given below, and more detailed remarks are given in section 2.

1.1.1 Ionization Decomposition and Transport

The ionization transport takes the charge deposited in an active volume within a TPC detector and transports it through the field cage structure of the TPC to the read-out plane. The charge which is deposited can either be generated externally, by GEANT or internally given knowledge about parameters of the the fill gas in the chamber such as the mean free path and ionization potential.

In the most common mode of operation, the ionization of the particle tracks will be described by GEANT, which will provide the amount of energy deposited (dE) over a given path-length (ds), by a particle with a momentum $\vec{p}$. Given the average ionization potential of the gas, the total number of electrons can be calculated such that the transport can be done at the segment level (dE) or the single electron level. This provides a mechanism which allows the possibility to distinguish between a detailed microscopic simulation and a macroscopic parameterization; that is, the granularity of the simulation can take on a range from the single electron level to a charge segment containing many 10s of electrons. By varying the length of the segment that is transported (and subsequently processed), the granularity of the simulation can be varied. The ionization can then be distributed on the pad-plane according to the distributions which characterize the effects of diffusion. The role of the charge transporter is to alter the x and y positions according to the transverse diffusions, the z position to reflect the drift time, with the effects of longitudinal diffusion folded in) and the amount of charge that actually reached the read-out plane.

1.1.2 Charge Collection and Amplification

Once the electrons arrive at the read-out plane, they must be collected by the individual anode/sense wires of the multi-wire proportional chamber (MWPC). This is where the avalanche process multiplies the signal of several 10s of electrons to several 10^3-10^5, depending on the potential on the wires. This operation is somewhat of a hybrid as it is really occurring within a container, however the processes occur in the amplification stage require the knowledge of the wire grid structure, and so the processes are incorporated here for an efficient implementation.

1.1.3 Analog Signal Generation

Once the charge is multiplied at the field wires of the MWPC, the amount of charge induced on the pads produces an analog signal which varies as a function of time. These events can be modeled via two processes:

- charge induction on the pads.
- charge sampling by the electronics.

Given the amount of charge on the wires and the geometry of the pad plane, the induced charge on any arbitrary pad can be calculated. From this quantity of charge, the signal at the output of the pre-amplifier/shaper can be determined given the response (i.e. transfer function) of the analog electronics. Although the time evolution of the signal that is developed on the wires is nearly entirely due to the motion of the positive ions away from the wire, the number of electrons produced provides a measure of the total amount of charge that is available to be induced on the pad plane. The shaping width of the electronics provide an estimate of the fraction of charge that is really observed. In reality only a fraction of the total charge is seen because of the small mobility of the positive charged ions and it takes a long time for the signal to finally decay (the famous 1/T tail). As such the shaping properties of the analog electronics (i.e. pre-amplifier and pulse shaping) plays an important role in the amount of charge actually measured. As such, given the total amount of charge induced on the pads, the electronics will differentiate the signal, and be sensitive to a certain fraction of the total charge. In the case of STAR, it is of the order of 45% of the charge. This analog charge can then be distributed into time bins modeling the behavior of the switch capacitor array (SCA)

1.1.4 Digital Signal Generation

After the analog charge has been distributed into the time bins on each pad, it can be digitized. This is an important property which is to be modeled because STAR uses a non-linear 8-bit ADC which contains the information of a 10-bit linear scale. Both the analog and digital signal generation components operate on the signals which are distributed in time bins, however there functions and operations as well as the information contained differ enough to justify breaking the processes into two distinct types of processes. The digital information can be compressed much more and require a format that is accessible via the *Data Decoder.*[2]

[2] see DAQ interface to Offline, M. Shultz et al.

1.2 Data Containers

The containers required for **TRS** are essentially defined by the physics processes as described in section 1.1. Container classes are used rather than simple data structures because it is more simple to incorporate book-keeping and simple functions which are closely matched to the structure of the container into a class. In essence the containers establish a kind of *I/O* interface between the separate processes and allow the same "physics framework" to exist, independent of the granularity or detail of the simulation. As a concrete example the physics of the ionization transport of a charge segment through the TPC field cage is independent of whether the segment in question is a single electron or macroscopic charge cloud. As such the containers are designed in a very generic manner that would facilitate implementation of the physics processes at various levels of detail and granularity. The containers required for **TRS** are:

- *Charge Segment* – the input to the program is an amount of energy (dE) deposited in a TPC volume with length (ds), by a particle of momentum $\vec{p}$. In essence it is a object definition of a *g2t_tpc_hit*-like structure.
- *Charge Mini Segment* – a fraction of a Charge Segment (above) which can be, in the limit, the position of a single electron. This is transported to the read-out plane.
- *Wire Bin Entry* – Position and charge of an ionization segment (Charge Mini Segment) at the wire plane after the ionization transport.
- *Wire Histogram* – all anode/sense wires which make up the MWPC which facilitates the charge collection.
- *Analog Signal* – structure containing the time (centroid) and amplitude of a signal on a pad. This can function as storage for both analog and digital signals
- *Analog Sector* – contains analog signals on pads and is the main working structure for calculations involving the charge induced on the pads.
- *Digital Sector* – contains digital signals on pads and contains the output data of the simulation.

The containers and the processes are meant to be as independent as possible and only overlap when concerns of efficiency over ride the design guidelines. The functions of the containers are described in more detail below:

1.2.1 Charge Segment

The purpose of the slow simulator is to transform ionization segments (usually produced by GEANT, or some type of external program) to pixel, or Raw TPC Data. As such the input will nominally be a quantity of energy (dE) deposited by a track over a finite path length (ds) at a coordinate ($\vec{x}$). This information was previously wrapped in two C/Fortran structures called *g2t_tpc_hit* and *g2t_tpc_track*. In the context of **TRS** it is necessary, and more convenient, to have this data wrapped in a class structure. This allows the same possibilities of data access as simple structures, however the functionality goes beyond data encapsulation. It also allows the use of more flexible utilities such as the StThreeVector to keep track of the position and momentum of track segment, as well as the utilities these classes provide. Furthermore operations that are intrinsic to the segment itself such as rotation, fragmenting (segment splitting) (*Note:* splitting requires knowledge of the gas parameters as well), etc. can also be associated with the object making it more "complete". These operations are necessary for rotating the charge segment into the sector 12 reference frame of the TPC and splitting the ionization into smaller segments to increase the granularity of the simulation.

1.2.2 Charge Mini Segment

The charge mini segment is a fragment of a charge segment (above) after it has been split. It can contain the complete charge segment or a fraction of it. Each mini segment is distributed within the path length of the charge segment (ds) onto a helical trajectory according to the mean free path of the particle within the gas (medium). It is this mini segment on which the charge transporter *process* will operate. As such the relevant data members are the position of the segment and the number of electrons. Access and set functions are provided so that the transporter has read and write access to these quantities.

1.2.3 Wire Bin Entry

Once the charge reaches the anode wire grid it must be collected on the sense/anode wires. In order to distribute the ionization onto the wires after diffusion effects are introduced (in the charge transporter), the ionization must be repackaged such that a specific quantity of ionization can be assigned to a position on the anode wires. Thus the *wire bin entry* is made to collect an amount of charge, q in the vicinity of an anode wire at a position $\vec{x}$, which can be assigned to a wire.

1.2.4 Wire Histogram

The wire histogram is a class which models the charge collection on single wires in a controlled manner; that is, charge is assigned through the wire bin entry class. The functionality of this class goes beyond simply keeping track of the amount of ionization collected on a single wire, but also possesses functions necessary to calculate gas gain amplification of each cluster. The reason this *"process"* is associated with a container is that the structure and layout of the wire grid, which is necessary in the wire histogram is also necessary to be able to do gas gain. Thus instead of imposing overhead of redundant class construction, it was incorporated here. This is one of the advantages of Object-Oriented design. Each charge cloud can now be used to induce a signal on the pad plane.

1.2.5 Analog Signal

An electronic signal, regardless of it being analog or digital, can be characterized by a pair of numbers which represents the time (centroid) and total charge. This class provides both access and set functions to the data. The storage of an arbitrary signal is the purpose of this class. In order for full reconstruction of an analog form however, a functional form must also be specified. No matter, the final output of the **TRS** package is pixel data; that is a given amplitude at a given time which is indexed by a pad-row and pad number. Keeping the time allows the flexibility of zero-suppressing any data with a negligible amplitude. This structure is used to keep all the signals that are generated on the pad plane, both analog and digital. In this sense the term *analog* is probably a misnomer, but it is foreseen in the future to introduce another digital signal which does not require **float** precision of the stored values. This should improve the storage requirements for a single event.

1.2.6 Analog Sector

The final output of the simulator is pixel data which is indexed by pad-row, pad number, and perhaps time-bin. The sector is a container which can store an indeterminate number analog signals indexed by these quantities. As such after a specific charge is induced onto the cathode pads, the analog sector keeps track of all intermediate stages of calculation before digitization occurs. Please note that although both analog or digital signals can be stored, only analog information is stored within this structure. The data is accessible either by pad-row, or single pad indices. Iterators are also provided within the class to facilitate traversal of the structure.

1.2.7 Digital Sector

The final output of the simulator is pixel data which is indexed by pad-row, pad number. The digital sector is a container which can store an indeterminate number of digital (8-bit) signals indexed by these quantities. The complete simulation of a complete detector is 24 separate digital sectors.

2 Mode of Simulation

This section describes in detail the processes that are modeled, and the algorithms and methods that implement the physics.

2.1 Ionization Process

The classes that deal with the raw ionization components within the package is capable of manipulating ionization distributions either generated from an external package (i.e. GEANT), or given the momentum vector of a particle, generate the ionization in the active detector volume internally according to basic parameters of the fill gas in the chamber.

In normal operations, the ionization for each TPC sub-volume is taken according to the `g2t_tpc_hit` structures. This large segment is then broken up into pieces, according to an exponential distribution which has a mean value characterized by the mean free path, between ionizing interactions, of a charged particle within the gas. This distribution, which specifies the distance to the next interaction is given by:

$$f(d) = Ke^{-d/\bar{d}} \tag{2}$$

where $\bar{d}$ is the mean free path. It is derived from the number of ionizing collisions which occur per unit distance, $\bar{n}$. The mean free path is then given by $1/\bar{n}$. This gives rise to a distribution of ionizing interactions per unit distance which is Poissonian in character.

At each interaction point a single "primary" electron is produced. These electrons will have an energy distribution given by the Rutherford scattering formula. In the case of free e^-e^- scattering (or at high momentum transfer where the binding energy can be neglected), this implies an energy (E) distribution which varies as E^{-2}. Because the electrons are not, strictly speaking, free but rather bound to the atoms of the medium (in our case the TPC gas) via a finite potential, there is a modification to this energy dependence which is medium dependent. This dependence has been measured experimentally and can be quite accurately parameterized by a function of the form E^{-n}.[3] For Ar, it is found experimentally that n=2 is a good approximation. A similar behavior is expected for P10 which is 90% Ar. For lighter gases, n increases. For example, Ne requires n=2.2, and He, n=2.6. This "stiffening" of the primary electron energy spectrum is a consequence of the higher binding energies of the lighter gases, however it has the desirable effect of decreasing the width of the Landau distribution as lower Z gases are used. The reason is that although fewer secondary electrons are produced, the spread in the energy distribution is smaller, and this compensates for the degradation in statistics. For this reason, resolution of dE/dx measurements are nearly constant, independent of the gas type used (to first order).

The energy dependence of the primary electrons is important because it determines the amount of subsequent ionization that is generated. For those primaries that have an energy above the ionization potential of the medium, which is typically the order of 10s of eV, subsequent electrons (secondaries) can be generated. The number of secondaries N_{sec} is then given by:

$$N_{sec} = (E_p - I_p)/W \tag{3}$$

where E_p is the energy of the primary electron, I_p is the ionization potential of the medium and W is the amount of energy necessary to create an $e^- - ion$ pair. This is an "effective" quantity which is very difficult to calculate from first principles and therefore must be measured for each gas mixture individually. It is found that in most cases, except where the energy of the particle is very small, the amount of energy required to produce an $e^- - ion$ pair is independent of the energy of the incident particle. This is seen in figure 1.[4]

The total number of electrons produced per interaction is then given as the sum of the primaries and secondaries. Thus calculating the number of electrons generated in a specific length convolutes two distributions—a Poissonian which determines the number of interactions, and an E^{-n} which determines the majority of the yield. This procedure results in a Landau-like distribution—which is expected for the yield of ionization in a given path length. Results for Ar and Ne are shown in figure 2. Once the ionization is generated, or distributed into smaller segments, it may then be transported to the multi-wire proportional chamber (MWPC).

[3]see: H. Fischle et al., NIM **A301** (1991) 202; and B. Lasiuk NIM **A409** (1998) 402.

[4]From W. Blum and L. Rolandi *Particle Detection with Drift Chambers* Springer-Verlag 1994.

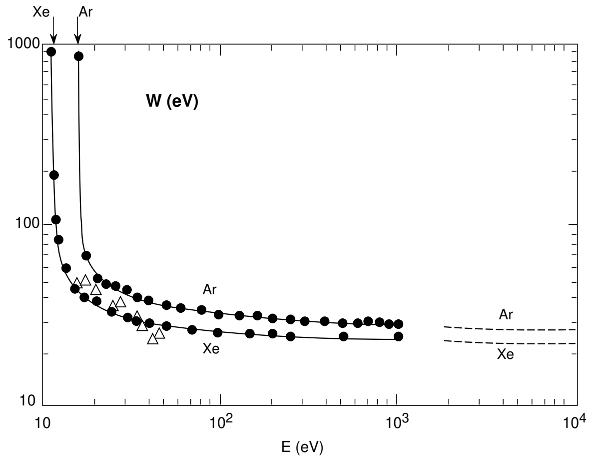

Figure 1: The average energy W spent (in eV) for the creation of one electron-ion pair in Ar and Xe as a function of the incident energy of the ionizing particle (in this case, an electron). Dashed lines are extrapolations to higher energies.

2.2 Charge Transporter

The charge, or ionization, in the segments that have been produced must be transported to the sense (anode) wires of the MWPC for read-out. This transport is modeled in the **Charge Transporter** component of **TRS**, and three distinct processes are described:

- E $\times$ B Effect.
- Transverse and Longitudinal Diffusion.
- Charge Loss *through*
  - Absorption through attachment (O_2).
  - Gating Grid Transparency.

and it is possible to control each process independently. The charge transporter calculates the position of the charge segment/electron at the z-plane of the anode/sense wire grid and the amount of charge that arrives. This charge must then be collected and amplified on the anode wires. In the current implementation (i.e. *FAST*) the charge is simply projected in the z coordinate to the position of the anode/sense wire plane; the underlying assumption that the ionization follows the $\vec{E}$ field lines and no distortions are visible. This will be refined in future versions.

2.2.1 E $\times$ B Effect

NOTE: not currently implemented!

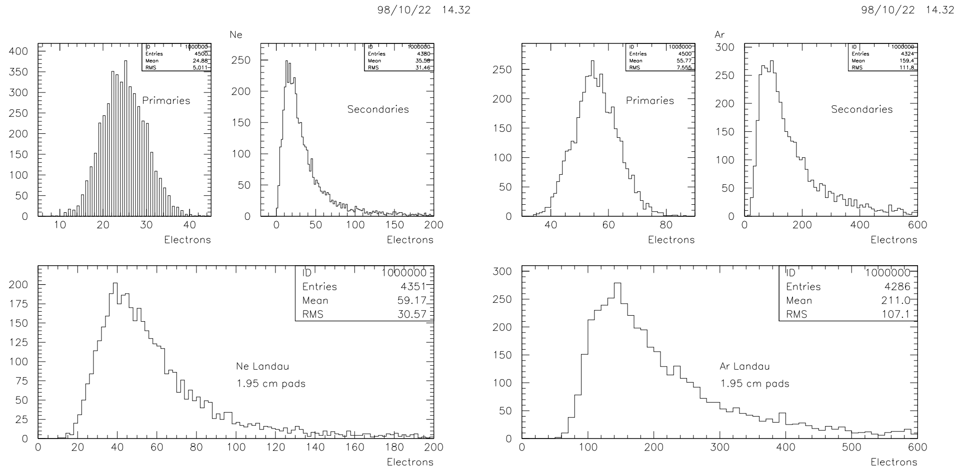

Figure 2: Ionization statistics for primary, secondary, and total yield distributions for Ne (left panel) and Ar (right panel). All yields are from a path length of 1.95 cm which is the pad length in the outer part of the TPC super-sector.

A misalignment between the electric and magnetic fields or inhomogeneities in the magnetic field can give rise to the ionization following trajectories which are not parallel to the $\vec{E}$ field lines. This introduces distortions into the trajectories of ionization left in the chamber. These are collectively known $\vec{E} \times \vec{B}$ distortions. In the general case of a charged particle in the presence of an electric and magnetic field, it will not follow a trajectory which is described by the Langevin equation:

$$\frac{d\mathbf{v}}{dt} = \frac{q}{m}(\mathbf{E} + \mathbf{v} \times \mathbf{B}) - \frac{1}{\tau}\mathbf{v} \tag{4}$$

where q is the charge of the particle, m is its mass, $\mathbf{v}$ is its velocity, $\mathbf{E}$ the electric (drift) field, $\mathbf{B}$ the magnetic field, and τ is the average time between collisions with the molecules in the medium. The last term is essentially a frictional force that limits the maximum average drift velocity. The steady state solution (i.e. $\frac{d\mathbf{v}}{dt} = 0$) is given by:

$$\mathbf{v} = \frac{\mu|\mathbf{E}|}{1 + \omega^2\tau^2}(\hat{\mathbf{E}} + \omega\tau(\hat{\mathbf{E}} \times \hat{\mathbf{B}}) + \omega^2\tau^2(\hat{\mathbf{E}} \cdot \hat{\mathbf{B}})\hat{\mathbf{B}}) \tag{5}$$

where μ ($= \frac{e\tau}{m}$) is the electron mobility and ω ($= \frac{eB}{m}$) is the cyclotron frequency. Although in the ideal field cage structure of a TPC, the electric and magnetic fields are parallel and the drift direction is defined by the electric field vector. Deviations from this idealization introduces velocity components in the orthogonal directions.

Equation 5 allows the drift velocity to be calculated at any arbitrary spatial point given knowledge regarding the electro-magnetic field vectors and the mobility of electrons in the gas. The distortions can then be modeled either by numerically integrating the equation over the drift time of the ionization, or parameterizing the displacement of the ionization in the plane orthogonal to the $\vec{E}$ field.

2.2.2 Diffusion

The effects of diffusion are due to thermal motion of the molecules in the gas and multiple scattering of the ionization in the transport from the position of deposition in the chamber to the read-out or sense wires on the pad plane. While the mean position of a charge segment may be transported through a volume with arbitrary electro-magnetic fields according to equation 5, its profile will broaden in proportion to the drift length, or more appropriately, the square root of its drift length. It is possible to parameterize the evolution of the size of the charge distribution (its width) in terms of a diffusion coefficient, which is in principle, different in the transverse (σ_T) and longitudinal (σ_L) directions. This distinction is important because the evolution of the diffusion coefficient in the transverse direction also depends on the presence of an magnetic field where it is reduced according to:

$$\sigma_{\mathbf{T}}(\mathbf{B}) = \frac{\sigma_T}{1+\omega^2\tau^2} \tag{6}$$

Once the charge segment/cloud is transported to the read-out plane, each segment (or sub-component) can be distributed according to a Gaussian (or any other) distribution characterized by a width derived from the diffusion constants. Increasing the granularity of the charge distribution will better reproduce single electron statistical fluctuations.

2.2.3 Charge Absorption

The absorption of charge is a complex process that can be attributed to many different mechanisms.[5] For our application we consider a simple parameterization of charge attachment in a gas where trace amounts of oxygen are present. The probability (P) for attachment to occur in a specified drift time, t, is given by:

$$P(t) = 1 - e^{-At} \tag{7}$$

where A specifies an *attachment rate* given by:

$$A = P_{O_2} \cdot P_M \cdot C_{O_2,M} \tag{8}$$

where P_{O2} and P_M are the partial pressures of the oxygen and TPC gas respectively. $C_{O2,M}$ specifies an *attachment coefficient* which is a function of the gas in question and the reduced electric field (E/p). For the case of STAR, a value of $C = 10.2\ \mu s^{-1}\ bar^{-2}$ has been deduced.[6] To give an idea of the order of magnitude, for a concentration of oxygen of 50 ppm and an ionization cloud drifting for 50 μs, the charge loss is expected to be approximately 2.5%. This charge loss can be applied at the single electron level or an extended charge cloud where a fraction of the total is lost.

[5] Details contained in a soon to be added appendix.

[6] soon to be added appendix.

2.2.4 Wire Grid Transparency

As the charge enters the region of the wire grids in the TPC, there is a non-zero probability that the charge may not be transmitted due to the potential configuration on the wire grids. In the STAR TPC there are three wire grids:

- anode/sense—responsible for charge collection and amplification.
- zero/frisch—defines the boundary of the field cage and allows a sink for ion collection in the amplification process.
- gate—switch which controls passage of ionization from the active TPC volume to the sense/anode wire plane.

The passage of ionization is controlled by the potential which is applied to the gate wires. Basically by setting the appropriate potential on this grid, the drift $\vec{E}$ lines can be made to terminate on the gating grid (zero transparency) or at the anode wires (full transparency). The transparency is the fraction of lines that terminate on the anode wires compared to those that terminate on the gating grid.

A general expression for the transparency of a mono-stable switched gating grid was deduced such that the full range from 0-100% transmission can be modeled. It should be noted that the effects of a bi-polar switching grid (which is the actual construction of the STAR-TPC) should not influence the values at more than the ~5% level. The expressions involved require only the geometry of the wire grids and the voltages set on the gating grid and high-voltage plane. An example of the transmission curve is shown in figure 3.

2.3 Charge Collection

According to the position of the charge segment/electron at the anode wire plane, the ionization can be collected by the nearest wire. The appropriate time delays for charge collection should a segment not be projected directly on top of the wire position can be calculated. Once the charge is assigned to a wire, the gas amplification can occur.

2.3.1 Gas Gain Amplification at Sense Wires

The process of gas amplification at the sense wires is modeled by the Raether distribution,[7] or, as it is denoted in Blum and Rolandi[8], the Yule-Furry process which describes the fluctuations in the amplification an amount of charge q with an exponential distribution:

$$p(q) = \frac{1}{\bar{q}} e^{-q/\bar{q}} \tag{9}$$

Subsequent theoretical refinements to this simple expression which were made in order to take into account effects like the asymmetric growth of the avalanche profile as well as saturation effects. This resulted in several distribution, the Polya distribution being the most popular. It requires an additional parameter to supplement the mean amplification

[7] see http://www.rhic.bnl.gov/STAR/html/comp_l/simu/TpcRespSim/src/literature.html

[8] W. Blum and L. Rolandi *Particle Detection with Drift Chambers* Springer-Verlag 1994.

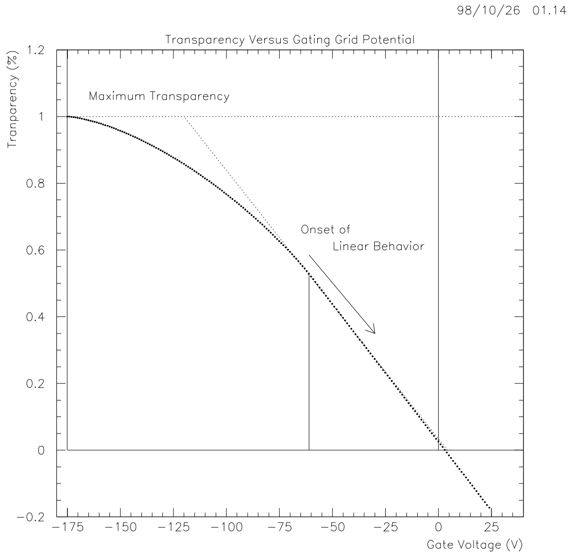

Figure 3: Wire Grid Transparency Calculation for nominal wire potentials and STAR outer sector read-out chamber geometry.

$(\bar{q})$. The effect of the additional parameter is to suppress the small amplification factors. As this parameter tends to zero, the Raether distribution is recovered. Experimentally, perfectly exponential behavior is seen at low to moderate gas gains (i.e.$<10^4$), in parallel plate geometry, however at gas gains above 10^5, slight deformation from exponential shape is observed. This is probably attributable to self-saturation effects which become important because of space charge. Since the TPC is generally operated at low gas gains, the simple Raether distribution was deemed acceptable, however the Polya function may be substituted if there is need.

It should be noted that in TPC (or any drift chamber) operation, the effect of the fluctuations in gas gain is to simply degrade the attainable space-point resolution, and for this purpose the exact functional form of the avalanche yields is not absolutely critical. This degradation is the physics that the implementation of the gas-gain fluctuations will attempt to address, and the Raether distribution should be quite acceptable in this regard.

Once the charge has been amplified, the amount of charge induced on the cathode pad plane can then be calculated.

2.4 Analog Signal Generation

The Analog Signal Generator has three main functions:

- Determine the charge induced on single pads from the charge "collected" on the anode wires.

- Sample the induced charge signals in time according to the electronics (i.e pre-amplifier/shaper) response.
- Distribute the **analog** charge into time bins according to the parameters of the switched capacitor array (SCA).

2.4.1 Charge Induction

The charge induced on a grounded pad plane by a point charge q located a distance d above the plane can be calculated by the method of images. The charge density (σ) on the plane is given by:

$$\sigma(x,y) = \frac{1}{2\pi} \frac{qd}{((x-x_o)^2 + (y-y_o)^2 + d^2)^{3/2}} \tag{10}$$

where the charge q is located at a position (x_o,y_o). However this expression is not the solution for the charge induced on the pad plane of a wire chamber. In the case of a MWPC the charge, which is at the position of the anode wire, is generally surrounded by *two* cathode planes—one from above and one from below.[9] Thus in order to calculate the charge density induced on the pad plane, all higher order multi-pole terms must be incorporated. This results in the following expression:

$$\sigma(x,y) = \frac{1}{2\pi} \sum_{n}^{\infty} \frac{(2n+1)qd}{((x-x_o)^2 + (y-y_o)^2 + ((2n+1)d)^2)^{3/2}} \tag{11}$$

Doing the sum, (and integrating over all y) yields a function which describes the charge distribution induced on the pad plane at a distance x from the wire where x_o is the position of the charge q:

$$\sigma(x,y) = \frac{q}{4d\cosh(\frac{\pi(x-x_o)}{2d})} \tag{12}$$

This function, an inverse hyperbolic cosine as shown in equation 12 is called an *Endo function.* Note that the derivation put no limits on the extent of the pad in the y direction (i.e. $\frac{w}{l} = 0$). The effect of finite geometry of segmented cathodes can be accounted for with the addition of another parameter. The same function can be written in a form more instructive for our purposes:

$$\sigma(x) = K_1 \frac{1 - \tanh^2(\frac{\pi(x-x_o)}{4d})}{1 + \tanh^2(\frac{\pi(x-x_o)}{4d})} \tag{13}$$

where K_1 is a normalization constant. Equation 13 can be used to generalize the Endo function in order to account for finite geometry effects of the segmented cathode pads. That

[9] Also the charge is in the form of a line charge associated with a linear charge density, not a discrete point charge.

is, each pad has a finite width/length ratio. This can be accounted for with the addition of another constant K_2:

$$F(x) = K_1 \frac{1 - \tanh^2(\frac{\pi(x-x_o)}{4d})}{1 + K_2 \tanh^2(\frac{\pi(x-x_o)}{4d})} \tag{14}$$

This is the generalized solution to the distribution of charge induced on a grounded pad plane by a point/line charge, and is usually dubbed, the Gatti function. The Gatti function is most prevalently used for pad chamber responses. Although more accurate, the price that is paid is the increase in time required to integrate equation 14 over the rather simple expression which can be deduced from the integral of 12 A comparison of the Gatti and Endo functions to a Gaussian (for reference) are given in figure 4

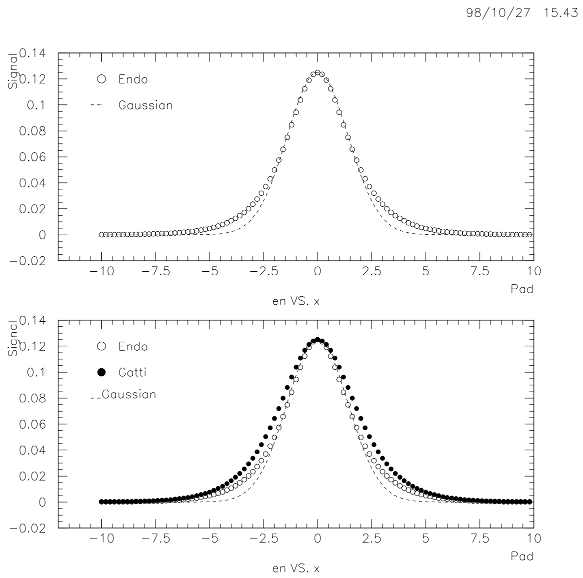

Figure 4: Comparison of Gaussian, Endo, and Gatti functions for profiles of the pad-response-function.

For the case of the TPC, the quantity of interest is the total amount of charge (Q) induced per pad which means one must integrate these functions, which specify the charge density, according to the pad dimensions. Thus for a point charge (equation 10), the integral is:

$$Q = \frac{1}{2\pi} \int_{yl}^{yu} \int_{xl}^{xu} dxdy \frac{qd}{((x-x_o)^2 + (y-y_o)^2 + d^2)^{3/2}} \tag{15}$$

where xl and xu denotes the lower and upper bounds of the pad in the x direction respectively. Similarly yl and yu denotes the same in the y direction. Similar integrals can be constructed given any arbitrary charge density (σ). The advantage of using such functions is that they allow the production of longer tails which have non-Gaussian characteristics. The tails are an important characteristic to understand as they determine the efficiency of the ionization collection which is very important in the study of ionization collection for $\frac{dE}{dx}$ resolution. Furthermore these integrals are well defined given the the position of the charge and the coordinates of the pads. Thus charge induced on adjacent pads as well as rows can be also be calculated quite simply in this formalism. Illustrations of some of these function are shown in figures 4.[10]

Please keep in mind that the fact that the signal on the wire is due almost exclusively to the motion of the charged ions **away** from the wire. In order to calculate the total amount of charge induced on the pad however, it is possible to use the number of electrons as a quantity, even though they are not the physical reason for the charge induction. This point will be reiterated in the electronics response of this description.

2.4.2 Sample the Signal in Time

Once the amount and centroid of the charge distribution on each pad is determined, this charge can be sampled in time corresponding to the analog electronics response. The signals are generated by super-imposing each analog signal from each avalanche which induces a signal on the pad plane. This allows the shaping time of the electronics can be varied independently of the width of the pad response function which is the strength of this simulation methodology. Currently four types of sampling are possible:

- delta function.
- Symmetric Gaussian.
- Asymmetric Gaussian.
- Parameterized STAR response.

A function also exists where a fractional scale of the total charge integral can be added as an Undershoot/Unrestored baseline component in the signal which has the effect of convoluting effects from the long 1/T tail. This is an important point and one that actually blurs the line of physics and simulation. In reality the time evolution of the signal that is developed on the wires is nearly entirely due to the **motion of the positive ions** away from the wire. This produces a signal with a long 1/T tail. For the STAR geometry the signal is $\sim$62 μs. In order to make a detector faster, the signal is differentiated after a characteristic time—the shaping time of the pre-amplifier. Although the detector response becomes faster, the trade-off is that only a fraction of the total charge is seen by the downstream electronics (i.e. the ADC). This fraction F, is given by:

$$F = \frac{ln(1+\frac{t_m}{t_o})}{ln(1+\frac{t_s}{t_o})} \tag{16}$$

where t_m is the length of time the undifferentiated signal would persist (i.e. $\sim$62 μs), t_o is the characteristic time of the signal development (i.e. $\sim$1 ns), and t_s is the shaping time

[10] For more details see: http://www.rhic.bnl.gov/STAR/html/comp_l/simu/TpcRespSim/src/literature.html

of the pre-amplifier (i.e. ~180 ns). For STAR this implies the order of 45% of the charge is distributed into time bins by the SCA. More importantly is that the signal shape is dominated very strongly by the shaping properties of the electronics. Thus the long time response of the chamber is parameterized in the electronics processing component of the simulator, rather than modeling the motion of the positive ions.

The symmetric Gaussian response, with the effect of an unrestored baseline due to under/over shoot is illustrated in figure 5 where the time evolution of a series of 20 signals,

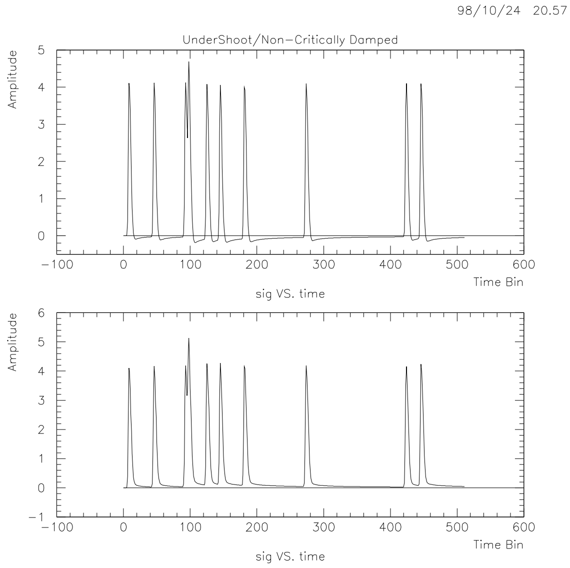

Figure 5: Asymmetric Gaussian Electronics Response with pedestal suppressed showing both undershoot (top panel) and an under damped baseline restoration (bottom panel).

of identical amplitude, are induced on a single pad.[11] The pulses are simply added using the principle of super-position. The modeling of an unrestored baseline is very important since the pulse height (actually the integral) of the signal is used as a measure of the velocity of the particle (via $\frac{dE}{dx}$ information). An unrestored baseline due to undershoot can result in an effective loss of charge in a high-multiplicity environment. Conversely an unrestored baseline due to under-damping will result in too much charge being observed at large drift distances. Both effects will reduce the attainable resolution if not taken into account.

Once the complete functional form of the signals induced on a pad over the read-out period of the TPC electronics, the analog charge can be distributed into discrete time bins. This sampling simulates the behavior of the switched capacitor array (SCA) in the front-end electronics. This is done by integrating the amount of charge in a time interval Δt, which is determined from the SCA sampling frequency. Chamber noise as well as electronic noise can be added at this point.

[11] More examples can be seen at: http://www.rhic.bnl.gov/STAR/html/comp_l/simu/TpcRespSim/src/literature.html

2.5 Digital Signal Generation

Once the analog charge is distributed into time bins on the pads, the digitization can occur. This is currently a simple conversion from voltage to ADC counts. Other features such as the addition of a pedestal and non-linearities in the ADC can also be added. In fact, any characteristic of the digital electronics can be added and will be independent of the analog signal sampling. This is very close to the way the front-end electronics are designed where the digital and analog electronic components are separated.

3 Physics Limitations

There are still some components either not implemented, or completely missing from TRS in its current form. It is hoped that these will be incorporated as the understanding of TRS evolves. Most critically is the noise. Although some preliminary work exists for this modeling, it has currently not reached a mature enough state where it can be added. Some obvious short-comings are listed below.

- $\vec{E} \times \vec{B}$ in not tested although code exists and can be "plugged" in.
- Noise at the chamber and electronics level does not yet exist.
- A function (or look-up table) is needed for the non-linear ADC response.
- The pad geometry is not incorporating the fractional pads at the border of the sectors.
- The gas gain is currently independent of the wire and the position of the avalanche on the wire.
- Effects of space charge in the charge transport stage of the simulation.
- No positional dependence in the transparency of the gating grid exists. Currently a constant transparency, independent of position is calculated.

It is almost certain that as experience is gained with the package, this list will be further expanded, however the code is written in a flexible manner such that these type of additions should be relatively straight forward.